

# Sensitivity of the Superconducting Transition Temperature to Changes in the Spin-Fluctuation Spectral Weight

P. McHale\* and P. Monthoux

*Cavendish Laboratory, University of Cambridge*

*Madingley Road, Cambridge CB3 0HE, United Kingdom*

(February 1, 2008)

## Abstract

In the simplest model of magnetic pairing, the transition temperature to the superconducting state depends on the dynamical susceptibility  $\chi(\mathbf{q}, \omega)$ . We discuss how  $T_c$  is affected by different momentum and frequency parts of  $\chi(\mathbf{q}, \omega)$  for nearly antiferromagnetic and nearly ferromagnetic metals in two dimensions. While in the case of phonon-mediated superconductivity any addition of spectral weight to  $\alpha^2 F(\omega)$  at  $\omega > 0$  leads to an increase in  $T_c$ , we find that adding magnetic spectral weight at any momentum  $\mathbf{q}$  and low frequencies ( $[0 : 3T_c]$  and  $[0 : (5 - 9)T_c]$  for nearly antiferromagnetic and ferromagnetic metals respectively) leads to a suppression of  $T_c$ . The most effective frequency and momentum range consists of large momenta  $\mathbf{q} \sim (\pi, \pi)$  and frequencies around  $10T_c$  for nearly antiferromagnetic metals and small momenta  $\mathbf{q} \sim 0$  and frequencies of approximately  $(13 - 22)T_c$  for

---

\*Present address: Max-Planck-Institut für Physik komplexer Systeme, Nöthnitzer Str. 38, 01187 Dresden, Germany

nearly ferromagnetic metals.

PACS Nos. 74.20.Mn

## I. INTRODUCTION

In principle there are over one million ternary and over one hundred million quaternary crystalline materials. Even the binary compounds number well over eleven thousand. Only a tiny percentage of these materials have been synthesised. Clearly an exhaustive search of the periodic table for superconductivity is out of the question. However, there exist in nature a wide range of compounds which are very close to a magnetic instability, and in quite a number of cases, an anisotropic superconducting phase is experimentally found on the border of magnetic order. But this type of superconductivity is sometimes confined to very small regions of the phase diagram, making it difficult to detect. The heavy-fermion superconductor  $\text{UGe}_2$ <sup>1</sup> is a case in point. An intuitive understanding of the trends in  $T_c$  not only provides a test of our models of anisotropic superconductivity but can also guide the experimental search for new anisotropic superconductors.

One of the most extensively investigated models of anisotropic superconductivity is based on a magnetic interaction, in which quasiparticles interact via the exchange of ferromagnetic or antiferromagnetic spin-fluctuations. An understanding of the properties of this model is essential in assessing its ability to describe metallic systems on the border of magnetic long-range order. The role of dimensionality, whether one is close to a ferromagnetic or antiferromagnetic instability and the sensitivity of  $T_c$  to model parameters have been investigated within a mean-field framework.<sup>2,4,3</sup> In these calculations, the transition temperature reflects an integral property of the magnetic excitation spectrum and does not tell us how much different parts of  $\chi(\mathbf{q}, \omega)$  contribute to the answer.

For the traditional isotropic superconductors, the transition temperature  $T_c$  depends upon the spectral function  $\alpha^2 F(\omega)$  which characterises the phonon-mediated electron-electron interaction. The sensitivity of the transition temperature to variations in the spectral distribution  $\alpha^2 F(\omega)$  was first investigated by Bergmann and Rainer<sup>5</sup>. They found that all frequency regions of  $\alpha^2 F(\omega)$  yield a positive contribution to  $T_c$ . Frequencies  $\omega \gg T_c$  and  $\omega \ll T_c$  contribute little (nothing in the limit  $\omega \rightarrow 0$ ) while frequencies around  $2\pi T_c$

contribute the most.

Later Millis, Sachdev and Varma<sup>8</sup> extended the Bergmann-Rainer analysis of the Éliashberg equations to the case of magnetically mediated singlet superconductivity. They assumed that the dynamical magnetic susceptibility could be expressed as a momentum-dependent factor times a frequency-dependent factor and that the spin fluctuations could be described by an Einstein model. In their model the sensitivity of  $T_c$  to changes in the magnetic spectral weight did not depend on the paramagnon momentum  $\mathbf{q}$  and made the computational analysis of the problem very similar to that of the phonon case. They showed that, in contrast to the latter problem, there is a crossover frequency  $\omega_{cross}$  such that adding magnetic spectral weight at frequencies  $\omega < \omega_{cross}$  led to a reduction in  $T_c$ .

More recently, Monthoux and Scalapino<sup>6</sup> carried out this analysis for the fluctuation-exchange approximation to the two-dimensional Hubbard model. For this more realistic magnetic pairing interaction, which is very non-local in space, they generalized the Bergmann-Rainer approach in order to study how sensitive the transition temperature to the  $d_{x^2-y^2}$  superconducting state is to infinitesimal changes in the spectral weight at frequency  $\omega$  and momentum  $\mathbf{q}$ . In agreement with the results of Millis et al<sup>8</sup>, they found that adding spectral weight at very low frequencies and for any momentum  $\mathbf{q}$  led to a reduction in  $T_c$ . They also found that there was a region in momentum space near  $\mathbf{q} = 0$  where any small addition of spectral weight at any frequency also led to a reduction in  $T_c$ . They mapped out the region in  $\mathbf{q}$  and  $\omega$  space that gave a positive contribution to  $T_c$ , essentially wavevectors near  $\mathbf{q} = (\pi, \pi)$  and frequencies  $\omega > T_c$ .

Here we report the results of a similar analysis using a parametrization of the effective interaction arising from the exchange of magnetic fluctuations. We consider systems on the border of antiferromagnetism and ferromagnetism. We study changes in  $T_c$  brought about by small variations in the spectral weight at some wavevector  $\mathbf{q}$  and frequency  $\omega$ . We map out the regions of wavevector and frequency space where a small addition of spin-fluctuation spectral weight yields an enhancement or suppression of  $T_c$ . This will give a more detailed understanding of the trends in  $T_c$  that one calculates from the model. We

shall contrast these findings with those obtained for the conventional phonon-induced pairing mechanism<sup>5</sup> to gain insights into the similarities and differences between phonon-mediated and magnetically mediated superconductivity.

## II. MODEL

We consider quasiparticles on a two-dimensional square lattice and postulate the following effective action

$$S_{eff} = \sum_{\mathbf{p}\alpha} \int_0^\beta d\tau \psi_{\mathbf{p}\alpha}^\dagger(\tau) (\partial_\tau + \epsilon_{\mathbf{p}} - \mu) \psi_{\mathbf{p}\alpha}(\tau) - \frac{g^2}{6N} \sum_{\mathbf{q}} \int_0^\beta d\tau \int_0^\beta d\tau' \chi(\mathbf{q}, \tau - \tau') \mathbf{s}(\mathbf{q}, \tau) \cdot \mathbf{s}(-\mathbf{q}, \tau'), \quad (1)$$

where  $\psi_{\mathbf{p}\sigma}^\dagger$  and  $\psi_{\mathbf{p}\sigma}$  are Grassman variables and  $N$  is the total number of allowed wavevectors in the Brillouin Zone. The spin density is given by

$$\mathbf{s}(\mathbf{q}, \tau) \equiv \frac{1}{N} \sum_{\mathbf{p}\alpha\gamma} \psi_{\mathbf{p}+\mathbf{q}\alpha}^\dagger(\tau) \boldsymbol{\sigma}_{\alpha\gamma} \psi_{\mathbf{p}\gamma}(\tau), \quad (2)$$

where  $\boldsymbol{\sigma}$  is the vector whose components are the three Pauli spin matrices.

The dispersion relation is

$$\epsilon_{\mathbf{p}} = -2t(\cos(p_x) + \cos(p_y)) - 4t' \cos(p_x) \cos(p_y), \quad t' \leq 0.5t, \quad (3)$$

where for simplicity we use units in which the lattice spacing is unity. For comparison with earlier work on this model<sup>2,4</sup> we set  $t' = 0.45t$  and adopt the value  $n = 1.1$  for the band filling.

We parametrize the retarded generalized magnetic susceptibility as:

$$\chi(\mathbf{q}, \omega) = \frac{\chi_0 \kappa_0}{\kappa^2 + \hat{q}^2 - i[\omega/\eta(\hat{q})]}. \quad (4)$$

where  $\kappa$  and  $\kappa_0$  are the inverse correlation lengths with and without strong magnetic correlations respectively. The correlation length is related to the pressure applied to the sample with  $\kappa^2 = 0$  coinciding with the quantum critical point. Let

$$\hat{q}_{\pm}^2 = 4 \pm 2(\cos(q_x) + \cos(q_y)). \quad (5)$$

For antiferromagnetic correlations the parameters  $\hat{q}^2$  and  $\eta$  are

$$\hat{q}^2 = \hat{q}_+^2 \quad (6)$$

$$\eta(\hat{q}) = T_{sf}\hat{q}_-, \quad (7)$$

where  $T_{sf}$  is a characteristic spin-fluctuation temperature. In the ferromagnetic case

$$\hat{q}^2 = \hat{q}_-^2 \quad (8)$$

$$\eta(\hat{q}) = T_{sf}\hat{q}_-. \quad (9)$$

We obtain the total spin-fluctuation propagator on the imaginary axis  $\chi(\mathbf{q}, i\nu_n)$  via the spectral representation

$$\chi(\mathbf{q}, i\nu_n) = - \int_{-\infty}^{+\infty} \frac{d\omega}{\pi} \frac{\text{Im}\chi(\mathbf{q}, \omega)}{i\nu_n - \omega}. \quad (10)$$

To get  $\chi(\mathbf{q}, i\nu_n)$  to decay as  $1/\nu_n^2$  as  $\nu_n \rightarrow \infty$ , as it should, we introduce a cutoff  $\omega_{cut}$  and take  $\text{Im}\chi(\mathbf{q}, \omega) = 0$  for  $\omega \geq \omega_{cut}$ . A natural choice for the cutoff is  $\omega_{cut} = \eta(\hat{q})\kappa_0^2$ .

Using the effective action in Eq. (1) and the dynamical susceptibility in Eq. (10), the two-dimensional mean-field Eliashberg equations for the transition temperature  $T_c$  in the Matsubara representation reduce to

$$\Sigma(\mathbf{p}, i\omega_n) = g^2 \frac{T}{N} \sum_{\Omega_n} \sum_{\mathbf{k}} \chi(\mathbf{p} - \mathbf{k}, i\omega_n - i\Omega_n) G(\mathbf{k}, i\Omega_n) \quad (11)$$

$$G(\mathbf{p}, i\omega_n) = \frac{1}{i\omega_n - (\epsilon_{\mathbf{p}} - \mu) - \Sigma(\mathbf{p}, i\omega_n)} \quad (12)$$

$$\begin{aligned} \lambda(T)\Phi(\mathbf{p}, i\omega_n) &= \begin{bmatrix} g^2/3 \\ -g^2 \end{bmatrix} \frac{T}{N} \sum_{\Omega_n} \sum_{\mathbf{k}} \chi(\mathbf{p} - \mathbf{k}, i\omega_n - i\Omega_n) \\ &\quad \times |G(\mathbf{k}, i\Omega_n)|^2 \Phi(\mathbf{k}, i\omega_n), \end{aligned} \quad (13)$$

where

$$\lambda(T) = 1 \Rightarrow T = T_c. \quad (14)$$

$\Sigma(\mathbf{p}, i\omega_n)$ ,  $G(\mathbf{p}, i\omega_n)$  and  $\Phi(\mathbf{p}, i\omega_n)$  are the Fourier components of the quasiparticle self-energy, the one-particle Green's function and the anomalous self-energy respectively. In Eq. (13) the prefactor  $-g^2$  is for singlet pairing while the prefactor  $g^2/3$  is for triplet pairing.

We find an instability to a d-wave gap function with  $\Phi(\mathbf{p}, i\omega_n)$  transforming as  $\cos(p_x) - \cos(p_y)$  in the nearly antiferromagnetic case and an instability to a p-wave gap function with  $\Phi(\mathbf{p}, i\omega_n)$  transforming as  $\sin(p_x)$  or  $\sin(p_y)$  in the nearly ferromagnetic case.

The momentum convolutions in Eqs. (11) and (13) were evaluated with the aid of a fast-Fourier-transform algorithm on a  $128 \times 128$  lattice. The corresponding frequency sums were carried out using the renormalisation group technique of Pao and Bickers<sup>7</sup>. Between 8 and 16 Matsubara frequencies are kept at each stage of the renormalization group procedure. The renormalization procedure is started at a temperature  $T_0 = 0.4t$  and the frequency sum cut-off used is  $\Omega_c \approx 20t$ . The renormalization procedure restricts us to discrete temperatures so that the point at which the condition in Eq. (14) is met must be determined by interpolation. The discrete temperatures were sufficiently close that a linear interpolation was adequate. The renormalization procedure afforded us considerable savings in computer time and storage requirements. Because of this we were able to carry out a thorough analysis of the dependence of our results on the spin-fluctuation coupling parameter  $g^2\chi_0/t$  and the inverse correlation length parameter  $\kappa^2$ .

To investigate how strongly the transition temperature is influenced by various frequency and momentum parts of the paramagnon spectral function, we add an infinitesimal amount of spectral weight at frequencies  $\omega_0 > 0$  and  $-\omega_0$  and wavevector  $\mathbf{q}^*$  and numerically calculate the change in  $T_c$ . More specifically, the paramagnon spectral weight is changed from  $\text{Im}\chi(\mathbf{q}, \omega)$  to  $\text{Im}(\chi(\mathbf{q}, \omega) + \delta\chi(\mathbf{q}, \omega))$  with

$$\text{Im}\delta\chi(\mathbf{q}, \omega) = \eta\pi\{\delta(\omega - \omega_0) - \delta(\omega + \omega_0)\}\frac{N}{N_{\mathbf{q}^*}}\sum_{\mathbf{q}_i^*}\delta_{\mathbf{q}, \mathbf{q}_i^*}, \quad (15)$$

where  $\eta$  is a positive infinitesimal dimensionless parameter. The sum over  $\mathbf{q}_i^*$  includes  $\mathbf{q}^*$  and those wavevectors in the Brillouin zone related to it by the symmetry operations of the lattice.  $N_{\mathbf{q}^*}$  is the number of such wavevectors including  $\mathbf{q}^*$  itself.  $N$  is the total number of

allowed wavevectors in the Brillouin zone.

In the Matsubara representation, the addition of this infinitesimal amount of spectral weight corresponds to changing the effective interaction  $V_{eff}(\mathbf{q}, i\nu_n) = g^2\chi(\mathbf{q}, i\nu_n)$  in Eqs. (11) and (13) to  $V_{eff} + \delta V_{eff}$  where

$$\delta V_{eff}(\mathbf{q}, i\nu_n) = \frac{\eta}{\chi_0} g^2 \chi_0 \frac{2\omega_0}{\omega_0^2 + \nu_n^2} \frac{N}{N_{\mathbf{q}^*}} \sum_{\mathbf{q}_i^*} \delta_{\mathbf{q}, \mathbf{q}_i^*}, \quad (16)$$

The total effective interaction thus depends on the parameters  $\kappa$ ,  $\kappa_0$ ,  $g^2\chi_0/t$  as well as the ratio  $\eta/\chi_0$ , and therefore so does  $T_c$ . For small  $\eta$ , one has

$$T_c(\eta/\chi_0, \mathbf{q}^*, \omega_0, \dots) = T_c(0, \mathbf{q}^*, \omega_0, \dots) + \frac{\eta}{\chi_0} \frac{dT_c}{d(\eta/\chi_0)}(0, \mathbf{q}^*, \omega_0, \dots) \quad (17)$$

where  $\dots$  denote all the other parameters in the problem. The quantity

$$\Delta T_c(\mathbf{q}^*, \omega_0) = \frac{\chi_0}{T_c} \frac{dT_c}{d\eta}(\mathbf{q}^*, \omega_0) \Big|_{\eta=0} \quad (18)$$

is a measure of how sensitive  $T_c$  is to an infinitesimal change in the value of  $\text{Im}\chi$  at  $(\mathbf{q}^*, \omega_0)$ .

We calculate this derivative using the finite-difference estimate

$$\frac{dT_c}{d(\eta/\chi_0)}(\mathbf{q}^*, \omega_0) \Big|_{\eta=0} \approx \frac{T_c(\eta/\chi_0, \mathbf{q}^*, \omega_0) - T_c(0, \mathbf{q}^*, \omega_0)}{\eta/\chi_0}. \quad (19)$$

The value of the parameter  $\eta/\chi_0$  must be chosen small enough, such that the function  $T_c(\eta/\chi_0)$  is approximately linear in the vicinity of  $\eta/\chi_0$ . But if  $\eta/\chi_0$  is chosen too small, then it becomes very difficult to obtain reliable numerical estimates of the differences in  $T_c$ . We found that  $\eta/\chi_0 = 4 \times 10^{-4} t$  was a good compromise in the nearly antiferromagnetic case. A smaller value of  $\eta/\chi_0$  was necessary for some of the nearly ferromagnetic results. In particular, we carried out the nearly ferromagnetic calculations for  $\kappa^2 = 0.5$  and  $g^2\chi_0/t = 10, 5$  and for  $g^2\chi_0/t = 30$  and  $\kappa^2 = 2, 3, 4$  with  $\eta/\chi_0 = 5 \times 10^{-5} t$ . We estimate that the accuracy with which we calculated the derivative  $dT_c/d\eta$  in all cases is of the order of a few per cent.

As in Reference<sup>8</sup>, we define a crossover frequency  $\omega_{cross}(\mathbf{q}^*)$  by  $\Delta T_c(\mathbf{q}^*, \omega_{cross}) = 0$ .



Similarly, one can define an optimal frequency  $\omega_{opt}(\mathbf{q}^*)$  as the frequency where  $\Delta T_c$  is maximum.  $\omega_{opt}(\mathbf{q}^*)$  then indicates which paramagnon frequency and wavevector  $\mathbf{q}^*$  contribute most to pairing.

In order to make a comparison with the corresponding electron-phonon problem it is instructive to define a mass renormalization parameter  $\lambda_Z$  and interaction parameter  $\lambda_\Delta$ . We define

$$\lambda_Z = \frac{\int_{-\infty}^{+\infty} \frac{d\omega}{\pi} < \frac{1}{\omega} \text{Im} V_Z(\mathbf{p} - \mathbf{p}', \omega) >_{FS(\mathbf{p}, \mathbf{p}')} }{< 1 >_{FS(\mathbf{p})}} \quad (20)$$

$$\lambda_\Delta = - \frac{\int_{-\infty}^{+\infty} \frac{d\omega}{\pi} < \frac{1}{\omega} \text{Im} V_\Delta(\mathbf{p} - \mathbf{p}', \omega) \eta(\mathbf{p}) \eta(\mathbf{p}') >_{FS(\mathbf{p}, \mathbf{p}')} }{< \eta^2(\mathbf{p}) >_{FS(\mathbf{p})}} \quad (21)$$

where

$$V_Z(\mathbf{q}, \omega) = g^2 \chi(\mathbf{q}, \omega) \quad (22)$$

and

$$V_p(\mathbf{q}, \omega) = -\frac{g^2}{3} \chi(\mathbf{q}, \omega) \quad (23)$$

$$\eta(\mathbf{p}) = \sin(p_x) \quad (24)$$

for p-wave spin-triplet pairing ( $\Delta \equiv p$ ) while

$$V_d(\mathbf{q}, \omega) = g^2 \chi(\mathbf{q}, \omega) \quad (25)$$

$$\eta(\mathbf{p}) = \cos(p_x) - \cos(p_y) \quad (26)$$

in the case of d-wave spin-singlet pairing ( $\Delta \equiv d$ ). In carrying out the frequency integrations, we omitted the cutoff which was used in Eq. (10). The approximate effect of the cutoff is to multiply  $\lambda_\Delta$  and  $\lambda_Z$  by a common factor which is weakly dependent on wavevector and  $\kappa^2$ . This can be ignored since we will only be interested in the quotient  $\lambda_\Delta/\lambda_Z$ . The Fermi-surface averages are given by

$$< \cdots >_{FS(\mathbf{p})} = \int \frac{d^2 p}{(2\pi)^2} \cdots \delta(\epsilon_{\mathbf{p}} - \mu) \quad (27)$$

$$< \cdots >_{FS(\mathbf{p}, \mathbf{p}')} = \int \frac{d^2 p}{(2\pi)^2} \frac{d^2 p'}{(2\pi)^2} \cdots \delta(\epsilon_{\mathbf{p}} - \mu) \delta(\epsilon_{\mathbf{p}'} - \mu) \quad (28)$$

In practice, we compute the Fermi-surface average with a discrete set of wavevectors on a lattice and we replace the delta function by a finite-temperature expression

$$\int \frac{d^2p}{(2\pi)^2} \longrightarrow \frac{1}{N} \sum_{\mathbf{p}} \quad (29)$$

$$\delta(\epsilon_{\mathbf{p}} - \mu) \longrightarrow \frac{1}{T} f_{\mathbf{p}}(1 - f_{\mathbf{p}}) \quad (30)$$

where  $f_{\mathbf{p}}$  is the Fermi function and  $N$  is the number of wavevectors in The Brillouin Zone. Note that  $\frac{1}{T} f_{\mathbf{p}}(1 - f_{\mathbf{p}}) \rightarrow \delta(\epsilon_{\mathbf{p}} - \mu)$  as  $T \rightarrow 0$ . We used  $T = 0.1t$  and  $N = 128^2$ . The finite temperature effectively means that van Hove singularities will be smeared out. The Fermi-surface average that appears in  $\lambda_Z$ , Eq. (20), plays a role similar to that of  $\alpha^2 F(\omega)/\omega$  in the case of phonon-mediated superconductivity.

### III. RESULTS

The model consists of the parameters  $g^2\chi_0/t$ ,  $T_{sf}/t$ ,  $\kappa_0$  and  $\kappa$ . It is found experimentally that  $T_{sf}\kappa_0^2$  is approximately constant. We shall use this relation to eliminate one parameter from the set and pick a representative value of the product  $T_{sf}\kappa_0^2$ . We put  $T_{sf} = \frac{2}{3}t$  which corresponds to a temperature of 1000 K if the bandwidth is 1 eV, and  $\kappa_0^2 a^2 = 12$  for comparison with earlier work carried out on this model<sup>2</sup>. To obtain a representative value for the dimensionless coupling parameter  $g^2\chi_0/t$ , we make use of the Stoner criterion. In the vicinity of the magnetic instability,  $g\chi_0(\mathbf{Q}, 0) \approx 1$ , where  $\chi_0(\mathbf{q}, \omega)$  is the usual tight-binding Lindhard susceptibility and  $\mathbf{Q}$  the ordering vector. With  $\chi_0(\mathbf{Q}, 0) \approx N(0) \approx \frac{1}{8t}$  where  $N(0)$  is the single-particle density of states at the Fermi level, the value of the coupling parameter  $g^2\chi_0/t$  obtained is about 10. We stress that this is only an order of magnitude estimate of the coupling parameter.

Figures 1 and 2 show  $\Delta T_c(\mathbf{q}^*, \omega_0)$ , Eq.(18), versus frequency  $\omega_0$  for several values of (a)  $g^2\chi_0/t$ , (b)  $\kappa^2$  and (c)  $\mathbf{q}^*$ . Figure 1 shows the results in the case of a nearly antiferromagnetic metal and Figure 2 shows the results in the case of a nearly ferromagnetic metal. By contrast to the phonon case where  $\Delta T_c$  is always positive, note that there are wavevectors

$\mathbf{q}^*$  for which  $\Delta T_c$  is always negative, which means that spectral weight at these wavevectors is deleterious to superconductivity. And if spectral weight is added at sufficiently small frequencies  $\omega_0$ ,  $\Delta T_c$  is negative for all wavevectors  $\mathbf{q}^*$ . Finally, note that the overall scale of  $\Delta T_c$  for nearly ferromagnetic systems is larger than that for nearly antiferromagnetic systems. This indicates a larger sensitivity of the relative changes in  $T_c$  with respect to changes in the spin-fluctuation spectral weight for nearly ferromagnetic systems.

Figure 3 is a representative plot of

$$\Delta T_c^+ = \max \left\{ \frac{\chi_0}{T_c} \frac{dT_c}{d\eta}, 0 \right\} \quad (31)$$

as a function of the wavevector  $\mathbf{q}^*$  at which spectral weight is added for several values of  $\omega_0/t$  and for a nearly antiferromagnetic metal.  $\Delta T_c^+$  indicates the region of momentum and frequency space where adding a small amount of spectral weight enhances the superconducting transition temperature. Figure 4 is a complementary plot for

$$\Delta T_c^- = \min \left\{ \frac{\chi_0}{T_c} \frac{dT_c}{d\eta}, 0 \right\}, \quad (32)$$

which indicates the region of momentum and frequency space where adding a small amount of spectral weight suppresses the superconducting transition temperature. These results should be compared with the corresponding plots, shown in Figures 5 ( $\Delta T_c^+$ ) and 6 ( $\Delta T_c^-$ ), for the nearly ferromagnetic case. We have chosen the values of  $\omega_0$  for graphs (a-c) to be less than  $\omega_{opt}$  (which, for these parameter values, is about  $2.5t$  in the nearly antiferromagnetic case and about  $0.32t$  in the nearly ferromagnetic case) and the values of  $\omega_0$  in graph (d) to be greater than  $\omega_{opt}$ . The region in wavevector space where  $\Delta T_c \geq 0$  grows monotonically with  $\omega_0$ , starting from zero when  $\omega_0 < \omega_{cross}$ , the crossover frequency corresponding to the incipient ordering wavevector. However the maximum value of  $\Delta T_c$  passes through an extremum at  $\omega_0 = \omega_{opt}$ , the optimal frequency corresponding to the incipient ordering wavevector. It is interesting to find that the size of the region  $\Delta T_c \geq 0$  is approximately the same in the nearly antiferromagnetic and nearly ferromagnetic cases if  $\omega_0$  is chosen close to the corresponding optimal frequency  $\omega_{opt}$ , and that it is a significant fraction of the total

area of the Brillouin Zone. This suggests that except for very small values of  $\kappa^2$ , the pairing occurs mostly through the short-ranged magnetic fluctuations. Comparing the values of  $\Delta T_c$  in the frequency and wavevector scans suggests that removing spectral weight from low frequencies may be an effective way to enhance  $T_c$ .

We show in Figure 7 plots of  $\Delta T_c^+$  for various values of  $\kappa^2$  in the nearly ferromagnetic case. The surfaces are very similar to one another in the small  $\kappa^2$  limit. This can also be seen in the  $\Delta T_c$  versus  $\omega_0$  curves. However, since our mean-field calculations are likely not accurate very close to the critical point for magnetic order, we cannot state categorically what the limiting values of  $\Delta T_c$  are. The  $\Delta T_c = 0$  contour in wavevector space is quite insensitive to the value of  $\kappa^2$ , but is, however, very sensitive to the value of  $\omega_0$ .

Figure 8 shows how the crossover frequency  $\omega_{cross}(\mathbf{q}^*)$  depends on the coupling constant  $g^2\chi_0/t$  and the correlation wavevector  $\kappa^2$ , for the optimum wavevector, namely  $\mathbf{q}^* = (\pi, \pi)$  for nearly antiferromagnetic systems and  $\mathbf{q}^* = (0, 0)$  for nearly ferromagnetic systems. The figure shows that  $\omega_{cross}(\mathbf{q}^*)$  when scaled by  $T_c$ , is more robust to changes in  $g^2\chi_0/t$  and  $\kappa^2$  in the nearly antiferromagnetic case than in the nearly ferromagnetic case. The value of  $\omega_{cross}$  in the nearly antiferromagnetic case is about  $3T_c$  which is quite close to the value  $2T_c$  obtained in the Hubbard model<sup>6</sup>. The value of  $\omega_{cross}$  in the nearly ferromagnetic case lies between  $5T_c$  and  $9T_c$ . It is interesting to observe that in the limit of small coupling and far away from the magnetic instability,  $\omega_{cross}/T_c$  seems to approach a value common to both the nearly antiferromagnetic and nearly ferromagnetic cases. Figure 8(a) indicates that, for  $\kappa^2 = 0.50$  in the nearly ferromagnetic case,  $\omega_{cross}/T_c$  seems to depend on  $T_{sf}$  and  $\kappa_0^2$  only through the product  $T_{sf}\kappa_0^2$ , which is found experimentally to be approximately constant. Therefore  $\omega_{cross}$  is roughly proportional to  $T_c$ . But, for the same parameters,  $T_c$  scales approximately linearly with  $T_{sf}^2$ . Hence, for  $\kappa^2 = 0.50$  in the nearly ferromagnetic case,  $\omega_{cross}$  scales approximately linearly with  $T_{sf}$ .

One would like to understand the nature of the crossover frequency  $\omega_{cross}$  in terms of phonon-problem-like parameters. Millis and coworkers<sup>8</sup> showed that, in the antiferromagnetic magnetic fluctuation case,

$$\omega_{cross}/T_c \sim e^{\frac{1}{\gamma_d}}, \quad (33)$$

where  $\gamma_d$  is a d-wave effective interaction constant  $\gamma_d = \frac{\lambda_d}{\lambda_Z}$ . They assumed that the dynamical magnetic susceptibility can be separated into a wavevector-dependent factor and a frequency-dependent factor and they adopted an Einstein model to describe the frequency-dependent factor. They further assumed that the Éliashberg equations can be reduced to equations involving Fermi-surface quantities only. A similar calculation can be carried out in the nearly ferromagnetic case yielding

$$\omega_{cross}/T_c \sim e^{\frac{1}{\gamma_p}}, \quad (34)$$

with  $\gamma_p = \frac{\lambda_p}{\lambda_Z}$ . The results of the more complete calculation described in Section II are compared with these expressions for  $\omega_{cross}/T_c$  in Figure 9. Since  $\gamma_\Delta$  ( $\Delta = p, d$ ) is not an independent parameter in our model, we calculated  $\log(\omega_{cross}/T_c)$  and  $1/\gamma_\Delta$  for various values of  $\kappa^2$ . One sees that the expressions given in Eqs. (33) and (34) are a poor approximation to the value of  $\omega_{cross}/T_c$  calculated from the Eliashberg equations. The dependence of  $\omega_{cross}/T_c$  on  $\gamma_\Delta$  is much weaker than  $e^{\frac{1}{\gamma_\Delta}}$  and is not even monotonic in the nearly antiferromagnetic case. This finding is consistent with the inability to obtain a simple analytic expression similar to that proposed by McMillan to represent the  $T_c$  calculated numerically via the Éliashberg equations<sup>2,4</sup>.

We show in Figure 10 the variation of the normalised optimal frequency  $\omega_{opt}(\mathbf{q}^*)/T_c$  with  $g^2\chi_0/t$  and  $\kappa^2$  in the nearly antiferromagnetic case, with  $\mathbf{q}^* = (\pi, \pi)$ , and nearly ferromagnetic case with  $\mathbf{q}^* = (0, 0)$ . In the nearly antiferromagnetic case  $\omega_{opt}$  is approximately a constant equal to  $10T_c$ , which is close to the value it takes in the Hubbard model<sup>6</sup>. It is also of the same order of magnitude as  $2\pi T_c$ , the value it takes in the electron-phonon problem<sup>5</sup>. In the nearly ferromagnetic case  $\omega_{opt}$  lies between  $13T_c$  and  $22T_c$ .

As shown by Bergmann and Rainer for the phonon problem<sup>5</sup>, it is instructive to compare the frequency dependence of the spectral function with that of  $\Delta T_c$ . The results for the nearly antiferromagnetic case and  $\mathbf{q}^* = (\pi, \pi)$  are shown in Figure 11 for various values of  $\kappa^2$ .

Figure 11 shows that in the small  $\kappa^2$  limit (strong coupling) the peak in the spectral weight lies below the optimum frequency  $\omega_{opt}$ , while for large  $\kappa^2$  (weak coupling) it lies above  $\omega_{opt}$ . This is analogous to the results of Bergmann and Rainer who found that the transverse phonon mode was below the optimum frequency  $\omega_{opt} = 2\pi T_c$  for strong coupling superconductors such as Hg and above  $\omega_{opt}$  for weak coupling superconductors such as In. The results of Figure 11 suggest an explanation for a maximum  $T_c$  as a function of  $\kappa^2$ . As  $\kappa^2 \rightarrow 0$ , while the d-wave component of the pairing interaction increases, the frequency at which the spin-fluctuation spectral weight is maximum becomes smaller than  $\omega_{cross}$ , the frequency below which addition of spectral weight produces a suppression of  $T_c$ .

One might have expected that the  $\kappa^2$  for which  $T_c$  is maximum would be such that the peak in the spin-fluctuation spectral weight coincides with  $\omega_{opt}$ . But for  $g^2\chi_0/t = 10$ , the maximum  $T_c$  is found at  $\kappa^2 \approx 0.35$ , while the match between the peak in the spectral weight and  $\omega_{opt}$  occurs for  $\kappa^2 \approx 1$ . The shift in the peak of  $\text{Im}V_d$  relative to  $\omega_{opt}$  allows one to understand the trends in  $T_c$ , but the arguments remain qualitative.

Since the location of the peak in the spectral function does not depend on the value of  $g^2\chi_0/t$  and our results show that the frequency  $\omega_{opt}$  is approximately constant in the nearly antiferromagnetic case, one does not gain new insights by looking at the frequency dependences of  $\text{Im}V_d(\mathbf{q}^*, \omega_0)$  and  $\Delta T_c(\mathbf{q}^*, \omega_0)$  for different coupling constants.

In the nearly ferromagnetic case, since  $\text{Im}\chi(\mathbf{q} \rightarrow 0, \omega) = 0$  for  $\omega \neq 0$ , one sees that the situation is quite different and thus the shape of the curves  $\text{Im}V_p(\mathbf{q}^*, \omega_0)$  and  $\Delta T_c(\mathbf{q}^*, \omega_0)$  for the optimum wavevector  $\mathbf{q}^* = 0$  will not be similar, unlike the phonon and nearly antiferromagnetic cases.

#### IV. DISCUSSION

Our results demonstrate a number of significant differences as well as similarities between the magnetic fluctuation- and phonon-pairing mechanisms. In the latter case, the interaction is local in space but non-local in time. This means that there should be almost no variation

of  $\Delta T_c(\mathbf{q}^*, \omega_0)$  with  $\mathbf{q}^*$  and therefore one only need worry about the dependence of  $\Delta T_c$  on frequency. In the case of magnetic pairing however, the interaction is non-local in both space and time and as a result  $\Delta T_c(\mathbf{q}^*, \omega_0)$  exhibits a dependence on both wavevector  $\mathbf{q}^*$  and frequency  $\omega_0$ .

In the phonon case<sup>5</sup>, addition of an infinitesimal amount of spectral weight at any non-zero frequency  $\omega_0$  results in an enhancement of  $T_c$ , with an optimum frequency of  $2\pi T_c$ . In the limit  $\omega_0 \rightarrow 0$ ,  $\Delta T_c \rightarrow 0$ , which is consistent with Anderson's theorem<sup>9</sup> for isotropic superconductors. On the other hand, for the magnetic interaction model, addition of spectral weight at sufficiently low frequencies results in negative values of  $\Delta T_c$ . The intuitive understanding of this result<sup>8</sup> is also related to Anderson's theorem. Very low frequency paramagnons effectively act as a static non-magnetic impurity potential that scatters the quasiparticles. For anisotropic superconductors, Anderson's theorem does not apply and the presence of non-magnetic impurities leads to a suppression of  $T_c$ . Also note that for certain wavevectors  $\mathbf{q}^*$ ,  $\Delta T_c(\mathbf{q}^*, \omega_0)$  is always negative, regardless of  $\omega_0$ .

There are also significant differences between the nearly antiferromagnetic and nearly ferromagnetic cases. For instance, the crossover frequency  $\omega_{cross}$  at which  $\Delta T_c(\mathbf{q}^*, \omega_0) = 0$  depends more weakly on the model parameters  $\kappa^2$  and  $g^2\chi_0/t$  in the nearly antiferromagnetic case than in the nearly ferromagnetic case. ( $\omega_{cross}$  is strongly dependent on  $\mathbf{q}^*$  in both cases.) Similarly, the optimum frequency  $\omega_{opt}$  at which  $\Delta T_c(\mathbf{q}^*, \omega_0)$  is maximum is more weakly dependent on the model parameters  $\kappa^2$  and  $g^2\chi_0/t$  in the nearly antiferromagnetic metals than in the nearly ferromagnetic metals. Moreover, the overall scale of  $\Delta T_c$  is much larger in the former case than in the latter, indicating a much greater relative sensitivity of  $T_c$  to changes in the spectral weight for nearly ferromagnetic systems.

Our results also show similarities between magnetically mediated and phonon-mediated superconductivity. In all cases, the shape of the  $\Delta T_c$  curves are monotonic with a single optimum frequency (for each wavevector) and, in the high-frequency regime and for wavevectors such that  $\Delta T_c > 0$ , the curves behave similarly. The decrease of  $\Delta T_c$  with increasing  $\omega_0$  approximately mirrors the change in the interaction parameters  $\lambda_\Delta$  as  $V_{eff} \rightarrow V_{eff} + \delta V_{eff}$ .

The relative positions of the peak  $\omega_{max}$  in the spectral weight  $\text{Im}V_d(\mathbf{q}^* = (\pi, \pi), \omega)$  and optimum frequency  $\omega_{opt}$  in the strong coupling limit where  $\omega_{max} < \omega_{opt}$  and weak coupling limit in which  $\omega_{max} > \omega_{opt}$  is similar in some respects to the findings of Bergmann and Rainer<sup>5</sup> for the phonon problem. In that case, the transverse phonon frequency is below the optimum one for strong coupling superconductors and above in the weak coupling case.

Figure 2(c) shows a feature that may partially explain the difficulty in observing superconductivity on the border of itinerant ferromagnetism. Our results (see Figure 2(c)) show that adding spectral weight at large wavevectors is detrimental to  $T_c$ . In other words, antiferromagnetic correlations act to suppress pairing in nearly ferromagnetic systems. In the presence of a lattice, one would generically expect some enhancement of the magnetic response at large wavevectors due to nesting features in the Fermi surface for nearly-half-filled electronic bands. As explained in References <sup>2,4</sup>, magnetic pairing on the border of long-range ferromagnetic order is not as robust as magnetic pairing in nearly antiferromagnetic systems. The antiferromagnetic correlations inherent to the presence of a crystal lattice tend to suppress magnetic pairing in nearly ferromagnetic systems, thus making it even more difficult to observe.

## V. OUTLOOK

The dependence of the superconducting transition temperature on model parameters and the role played by dimensionality for Ornstein-Zernike like spin-fluctuation spectra has been studied in some detail<sup>2,4</sup>. However, these calculations reflect an integral property of the dynamical susceptibility  $\chi(\mathbf{q}, \omega)$ . In this paper, we presented a study of how different regions in wavevector  $\mathbf{q}$  and frequency  $\omega$  individually contribute to  $T_c$ , giving us novel insights into the magnetic interaction model.

The calculations were carried out by adding infinitesimal amounts of spectral weight at different wavevectors and frequency and determining the resulting changes in  $T_c$  from the numerical solution of the Eliashberg equations. We stress that the work reported here



provides insight only into how different regions in  $\mathbf{q}$  and  $\omega$  contribute to pairing for the particular magnetic-fluctuation spectrum  $\chi(\mathbf{q}, \omega)$ , Eq. (10). One may infer certain trends in  $T_c$  for small changes in the spin-fluctuation spectrum, but it may not be warranted to extrapolate our results to large changes in the magnetic spectrum. Also, the calculations are carried out at  $T_c$ . They may give one some idea of how the robustness of pairing is affected as one goes below  $T_c$  and the electronic gap induces changes in the momentum and frequency structure of  $\chi(\mathbf{q}, \omega)$ , but this involves another extrapolation to large changes in the magnetic spectrum which may not be warranted.

We found that addition of spectral weight at or near the incipient ordering wavevector in the nearly antiferromagnetic and nearly ferromagnetic cases lead to an enhancement of  $T_c$ , except at low frequencies where it leads to a suppression of the superconducting transition temperature. However, addition of spectral weight far away from the incipient ordering wavevector results in a lowering of  $T_c$  regardless of frequency. These results are in stark contrast to those obtained for phonon-mediated superconductivity where addition of spectral weight at any non-zero frequency leads to an enhancement of the superconducting critical temperature.

The theoretical framework presented here to describe systems on the border of magnetism can be translated to describe systems on the border of other types of instabilities, such as charge-density-wave or ferroelectric instabilities. The same type of calculations could be carried out in those other cases, and compared to the results of this paper, shedding light on the similarities and differences between the many possible pairing mechanisms.

## VI. ACKNOWLEDGMENTS

We acknowledge the support of the Isaac Newton Trust, the Cambridge European Trust, the Robert Gardiner Memorial Scholarship and the EPSRC. P. McHale acknowledges the hospitality of the MPIPKS, Dresden where the text was completed. Finally we thank G.G. Lonzarich for discussions on these and related topics.

## REFERENCES

- <sup>1</sup> S.S. Saxena, P. Argawal, K. Ahilan, F.M. Grosche, R.K.W. Haselwimmer, M.J. Steiner, E. Pugh, I.R. Walker, S.R. Julian, P. Monthoux, G.G. Lonzarich, A. Huxley, I. Sheikin, D. Braithwaite, J. Flouquet, *Nature* **406**, 587 (2000).
- <sup>2</sup> P. Monthoux and G. G. Lonzarich, *Phys. Rev. B* **59**, 14598 (1999).
- <sup>3</sup> R. Arita and K. Kuroki and H. Aoki, *Phys. Rev. B* **60**, 14585 (1999); *J. Phys. Soc. Jap.* **69**, 1181 (2000).
- <sup>4</sup> P. Monthoux and G. G. Lonzarich, *Phys. Rev. B* **63**, 054529 (2001).
- <sup>5</sup> G. Bergmann and D. Rainer, *Z. Phys.* **263**, 59 (1973).
- <sup>6</sup> P. Monthoux and D. J. Scalapino, *Phys. Rev. B* **50**, 10339 (1994).
- <sup>7</sup> Chien-Hua Pao and N. E. Bickers, *Phys. Rev. B* **49**, 1586 (1994).
- <sup>8</sup> A. J. Millis and Subir Sachdev and C. M. Varma, *Phys. Rev. B* **37**, 4975 (1988).
- <sup>9</sup> P.W. Anderson, *Phys. Chem. Solids* **11**, 26 (1959).

## FIGURES

FIG. 1. Frequency dependence of  $\Delta T_c = \frac{\chi_0}{T_c} \frac{dT_c}{d\eta}$  for various values of (a) the coupling parameter  $g^2\chi_0/t$ , (b) the inverse correlation length  $\kappa^2$  and (c) the momentum transfer  $\mathbf{q}^*$  in the case of a nearly antiferromagnetic metal with a  $d_{x^2-y^2}$  superconducting state symmetry. The characteristic spin-fluctuation temperature is  $T_{sf} = 0.67$  and  $\kappa_0^2 = 12$ .

FIG. 2. Frequency dependence of  $\Delta T_c = \frac{\chi_0}{T_c} \frac{dT_c}{d\eta}$  for various values of (a) the coupling parameter  $g^2\chi_0/t$ , (b) the inverse correlation length  $\kappa^2$  and (c) the momentum transfer  $\mathbf{q}^*$  in the case of a nearly ferromagnetic metal with a p-wave superconducting state symmetry. The characteristic spin-fluctuation temperature is  $T_{sf} = 0.67$  and  $\kappa_0^2 = 12$ .

FIG. 3. Wavenumber dependence of  $\Delta T_c^+ = \min\{\frac{\chi_0}{T_c} \frac{dT_c}{d\eta}, 0\}$  for various values of  $\omega_0/t$  for a nearly antiferromagnetic metal with a  $d_{x^2-y^2}$  superconducting state symmetry. The other pertinent parameter values are  $g^2\chi_0/t = 30$  and  $\kappa^2 = 0.5$ .

FIG. 4. Wavenumber dependence of  $\Delta T_c^- = \min\{\frac{\chi_0}{T_c} \frac{dT_c}{d\eta}, 0\}$  for various values of  $\omega_0/t$  for a nearly antiferromagnetic metal with a  $d_{x^2-y^2}$  superconducting state symmetry. The other pertinent parameter values are  $g^2\chi_0/t = 30$  and  $\kappa^2 = 0.5$ .

FIG. 5. Wavenumber dependence of  $\Delta T_c^+ = \max\{\frac{\chi_0}{T_c} \frac{dT_c}{d\eta}, 0\}$  for various values of  $\omega_0/t$  for a nearly ferromagnetic metal with a p-wave superconducting state symmetry. The other pertinent parameter values are  $g^2\chi_0/t = 30$  and  $\kappa^2 = 0.5$ .

FIG. 6. Wavenumber dependence of  $\Delta T_c^- = \min\{\frac{\chi_0}{T_c} \frac{dT_c}{d\eta}, 0\}$  for various values of  $\omega_0/t$  for a nearly ferromagnetic metal with a p-wave superconducting state symmetry. The other pertinent parameter values are  $g^2\chi_0/t = 30$  and  $\kappa^2 = 0.5$ .

FIG. 7. Wavenumber dependence of  $\Delta T_c^+ = \max\{\frac{\chi_0}{T_c} \frac{dT_c}{d\eta}, 0\}$  for various values of the dimensionless parameter  $\kappa^2$  for a nearly ferromagnetic metal with a p-wave superconducting state symmetry. The other pertinent parameter values are  $g^2\chi_0/t = 30$  and  $\omega_0/t = 2$ .

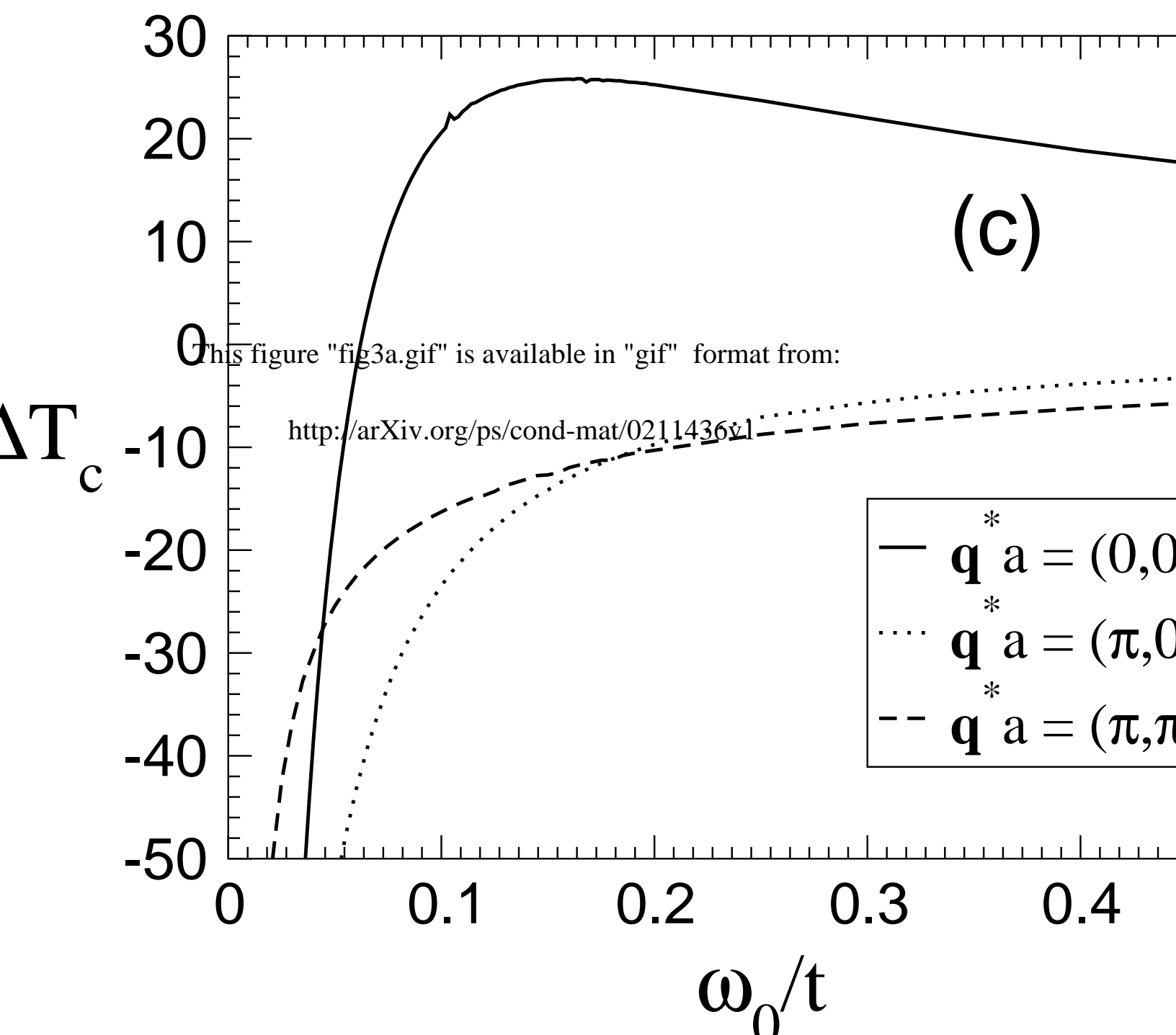
FIG. 8. The dependence of the crossover frequency  $\omega_{cross}$ , normalised by the superconducting transition temperature  $T_c$ , on (a) the coupling parameter  $g^2\chi_0/t$  and on (b) the inverse correlation length  $\kappa^2$ . Both graphs exhibit results obtained in the nearly antiferromagnetic (NA) case and for three values of the parameter pair  $(T_{sf}, \kappa_0^2)$ , keeping the product  $T_{sf}\kappa_0^2$  constant, in the nearly ferromagnetic (NF) case. Throughout we have put  $\mathbf{q}^* = (\pi, \pi)$  in the nearly antiferromagnetic case and  $\mathbf{q}^* = (0, 0)$  in the nearly ferromagnetic case.

FIG. 9. Comparison of our results for the crossover frequency in (a) the nearly antiferromagnetic case (circles) and (b) the nearly ferromagnetic case (circles) with the result  $\omega_{cross}/T_c \sim e^{\frac{1}{\gamma_\Delta}}$ , Eq. (33) (squares). We have put the prefactor in this formula equal to one for the sake of comparison. We have calculated  $\omega_{cross}$  with  $g^2\chi_0/t = 10$ , although the effective interaction constant  $\gamma_\Delta$  is independent of  $g^2\chi_0/t$ . The data is parametrised left to right by increasing  $\kappa^2$  from (a) 0.10 to 4.00 and (b) 0.10 to 1.00. Throughout we have put  $\mathbf{q}^* = (\pi, \pi)$  in the nearly antiferromagnetic case and  $\mathbf{q}^* = (0, 0)$  in the nearly ferromagnetic case.

FIG. 10. The dependence of the optimal frequency  $\omega_{opt}$ , normalised by the superconducting transition temperature  $T_c$ , on (a)  $g^2\chi_0/t$  and (b)  $\kappa^2$ . We have put  $T_{sf} = 0.67$ ,  $\kappa_0^2 = 12$  and  $\mathbf{q}^* = (\pi, \pi)$  in the nearly antiferromagnetic case and  $\mathbf{q}^* = (0, 0)$  in the nearly ferromagnetic case.

FIG. 11. Comparison of  $\Delta T_c = \frac{\chi_0}{T_c} \frac{dT_c}{d\eta}$  (solid line) and  $\text{Im}V_d$  (dashed line) for various values of the parameter  $\kappa^2$  for a nearly antiferromagnetic metal. The functions are plotted for a value of the coupling  $g^2\chi_0/t = 10$  and a wavevector  $\mathbf{q}^* = (\pi, \pi)$ .

$$g^2 \chi_0/t = 10; \kappa^2 = 0.50$$



This figure "fig3b.gif" is available in "gif" format from:

<http://arXiv.org/ps/cond-mat/0211436v1>

This figure "fig3c.gif" is available in "gif" format from:

<http://arXiv.org/ps/cond-mat/0211436v1>

This figure "fig3d.gif" is available in "gif" format from:

<http://arXiv.org/ps/cond-mat/0211436v1>



This figure "fig4a.gif" is available in "gif" format from:

<http://arXiv.org/ps/cond-mat/0211436v1>

This figure "fig4b.gif" is available in "gif" format from:

<http://arXiv.org/ps/cond-mat/0211436v1>

This figure "fig4c.gif" is available in "gif" format from:

<http://arXiv.org/ps/cond-mat/0211436v1>

This figure "fig4d.gif" is available in "gif" format from:

<http://arXiv.org/ps/cond-mat/0211436v1>

This figure "fig5a.gif" is available in "gif" format from:

<http://arXiv.org/ps/cond-mat/0211436v1>

This figure "fig5b.gif" is available in "gif" format from:

<http://arXiv.org/ps/cond-mat/0211436v1>

This figure "fig5c.gif" is available in "gif" format from:

<http://arXiv.org/ps/cond-mat/0211436v1>

This figure "fig5d.gif" is available in "gif" format from:

<http://arXiv.org/ps/cond-mat/0211436v1>



This figure "fig6a.gif" is available in "gif" format from:

<http://arXiv.org/ps/cond-mat/0211436v1>

This figure "fig6b.gif" is available in "gif" format from:

<http://arXiv.org/ps/cond-mat/0211436v1>

This figure "fig6c.gif" is available in "gif" format from:

<http://arXiv.org/ps/cond-mat/0211436v1>

This figure "fig6d.gif" is available in "gif" format from:

<http://arXiv.org/ps/cond-mat/0211436v1>

This figure "fig7a.gif" is available in "gif" format from:

<http://arXiv.org/ps/cond-mat/0211436v1>

This figure "fig7b.gif" is available in "gif" format from:

<http://arXiv.org/ps/cond-mat/0211436v1>

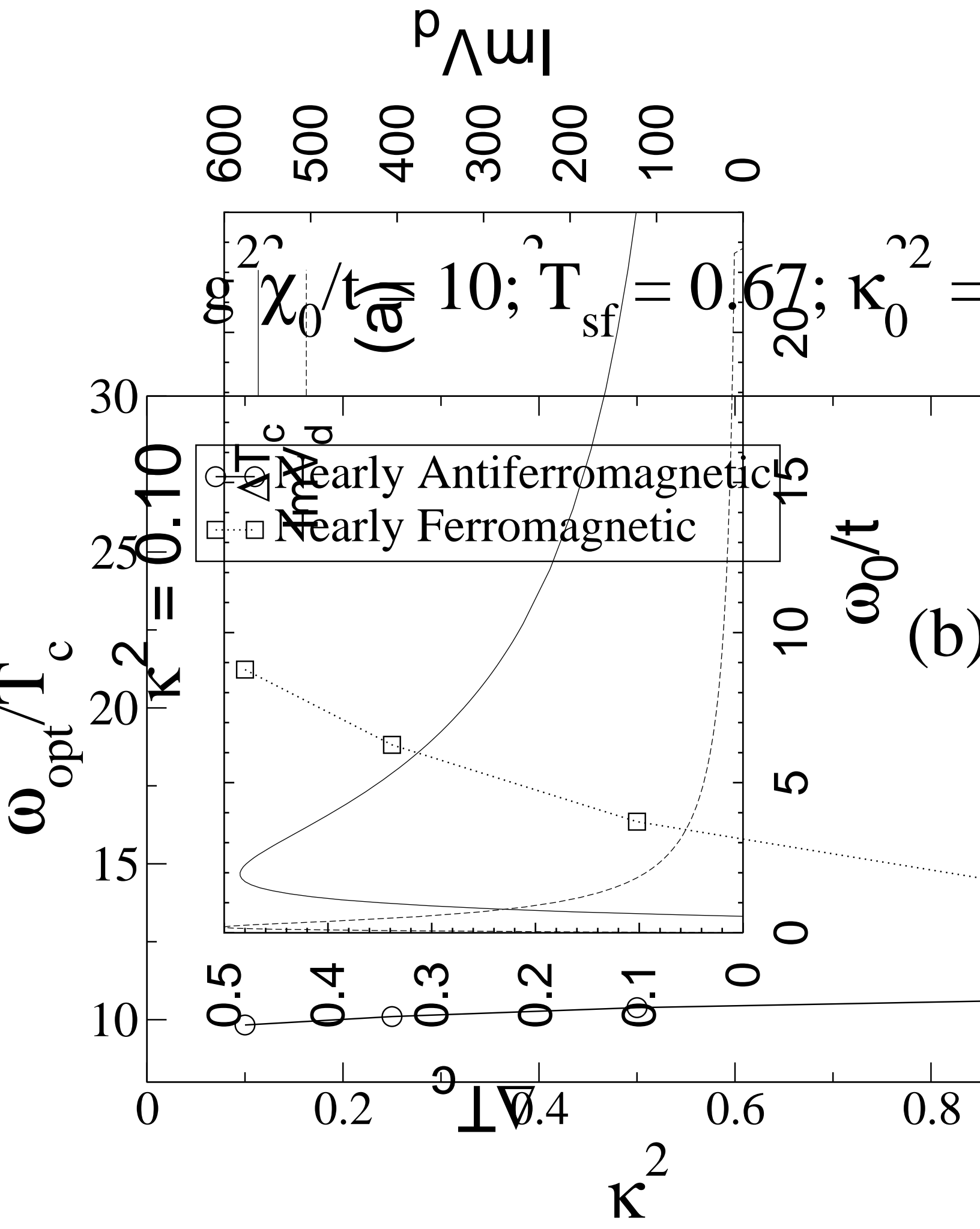
This figure "fig7c.gif" is available in "gif" format from:

<http://arXiv.org/ps/cond-mat/0211436v1>

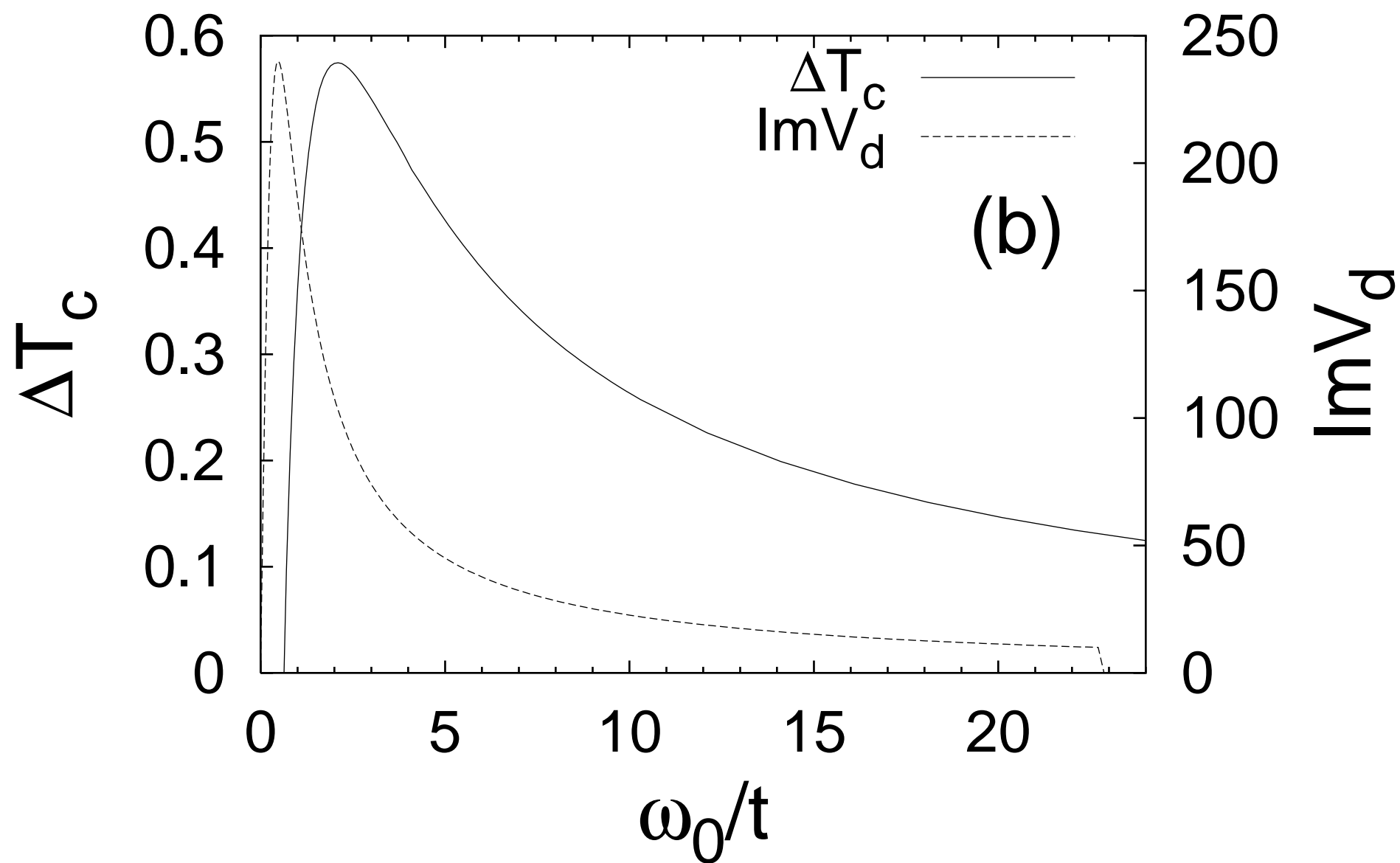
This figure "fig7d.gif" is available in "gif" format from:

<http://arXiv.org/ps/cond-mat/0211436v1>

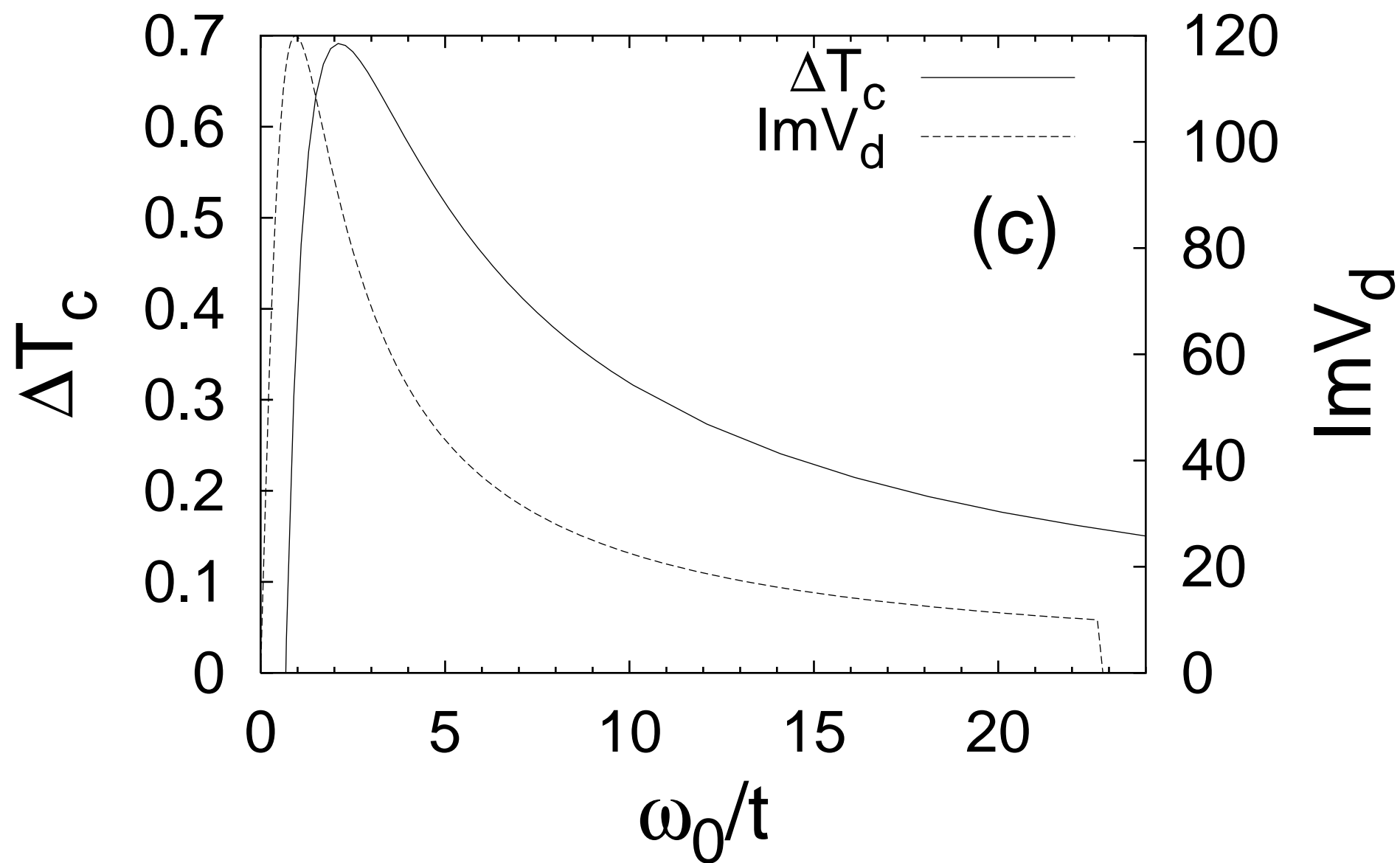




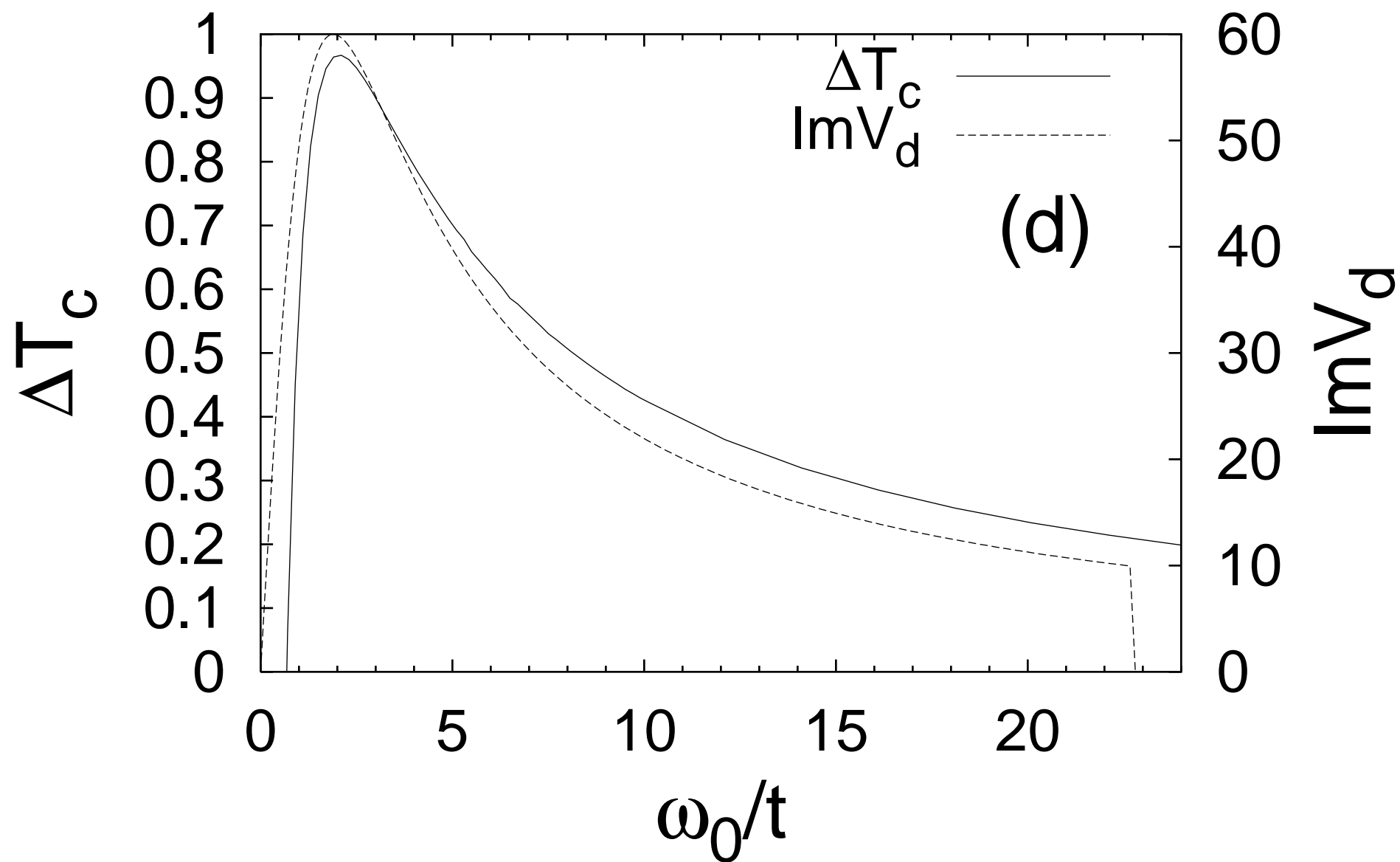
$$\kappa^2 = 0.25$$



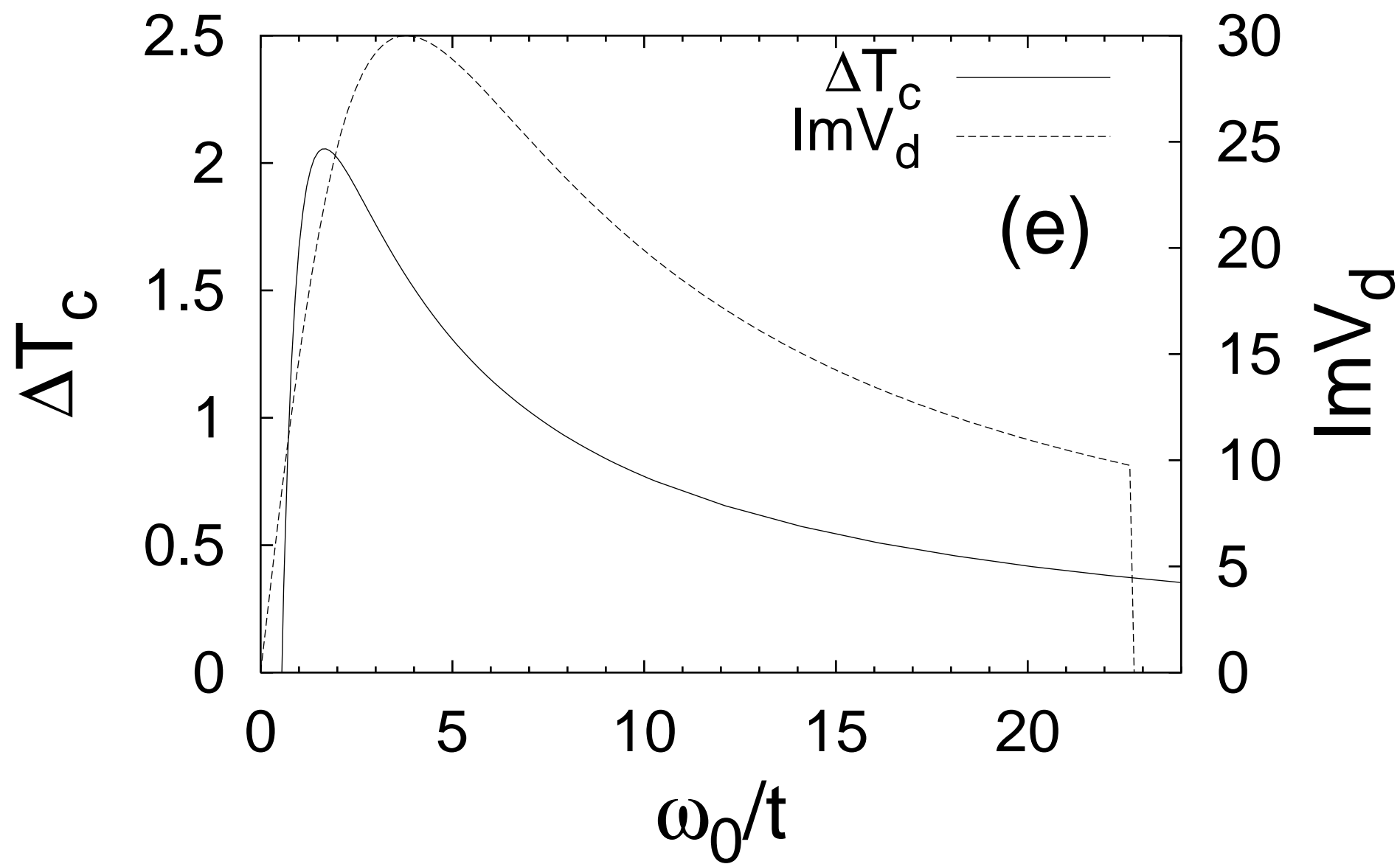
$$\kappa^2 = 0.50$$



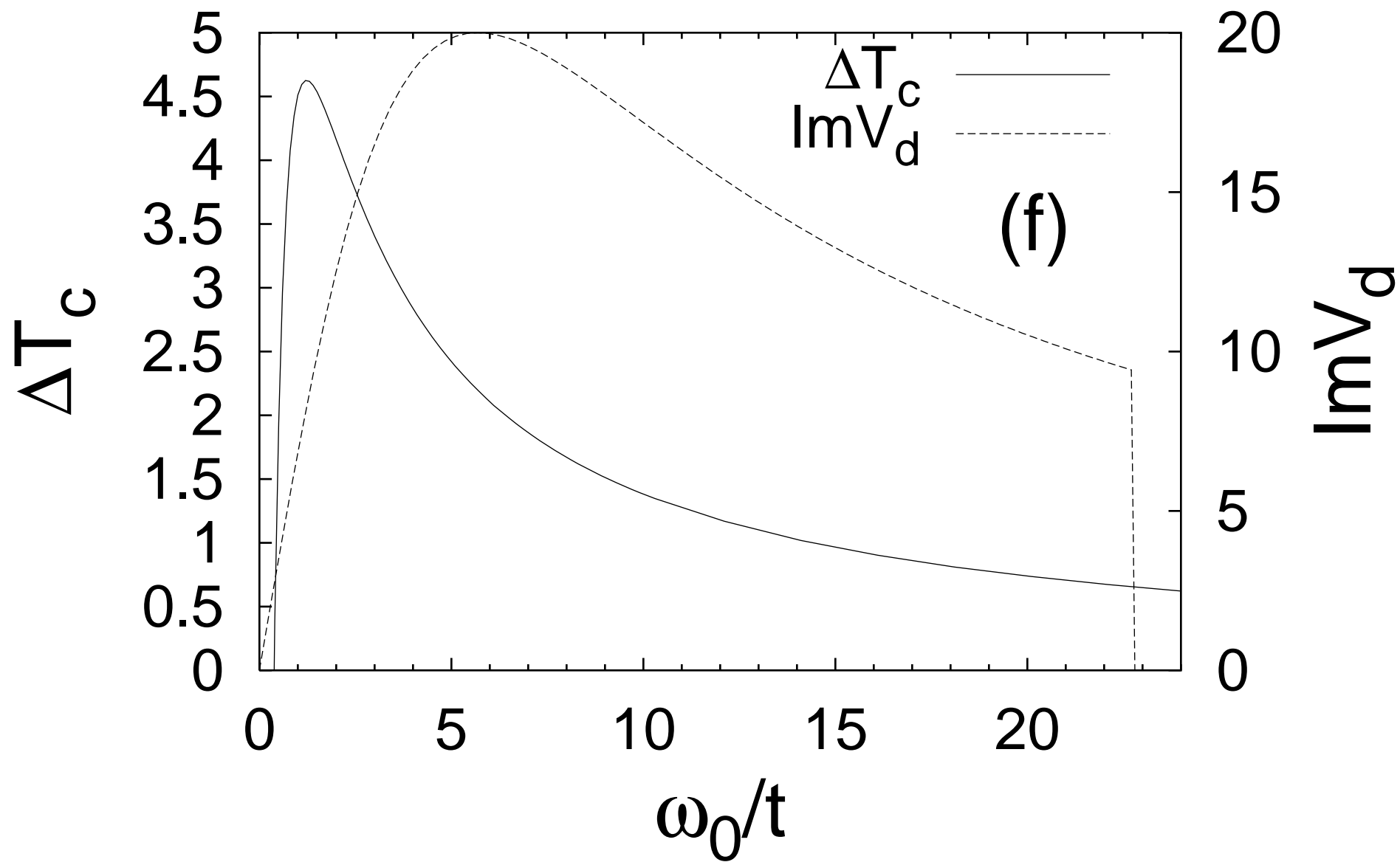
$$\kappa^2 = 1.00$$



$$\kappa^2 = 2.00$$



$$\kappa^2 = 3.00$$



$$\kappa^2 = 4.00$$

